TDDB AT LOW VOLTAGES: AN ELECTROCHEMICAL PERSPECTIVE

R. Muralidhar[1], T. Shaw[1], F. Chen[2], P. Oldiges[3], D. Edelstein[1], S. Cohen[1], R. Achanta[3], G. Bonilla[1] and M. Bazant[4]
[1]IBM Thomas J. Watson Research Center, Yorktown Heights, NY 10598 [2]IBM Microelectronics, Essex Junction, VT 05452;
[3]IBM Microelectronics, Hopewell Junction, NY 12533; [4]Department of Chemical Engineering,
Masachussets Institute of Technology, Cambridge, MA 02139
Phone: 914-945-1827; Fax: 914-945-4014; E-mail: muralidr@us.ibm.com

Abstract— TDDB lifetime projections at operating voltages for backend of line (BEOL) dielectrics have been based on accelerated testing at high fields and extrapolation to operating conditions based on electric field dependent dielectric wearout models. As operating voltages are reduced to 1V range, such intrinsic field acceleration based wearout mechanisms become negligible making such extrapolations questionable. At the same time, as we scale the BEOL geometries, extrinsic wearout mechanisms involving copper and moisture can impact TDDB reliability. In this paper, we, for the first time, investigate extrinsic reliability in low voltage regime where electro-chemical redox reactions are possible. We formulate a physical electrochemical model for TDDB. We present analytic solution for limiting cases that show TDDB lifetime dependence on voltage or electric field depending on relative rates of electrode reactions and field assisted ion transport. Generalization to higher voltages are also discussed.

Keywords: Low-field, TDDB, Electrochemical modeling

I. INTRODUCTION

As BEOL interconnect structures are scaled, denser insulator materials are replaced with porous low-K or Ultra-low k materials, and Copper barrier layers are thinned, time dependent dielectric breakdown (TDDB) is becoming a more significant reliability concern. In using accelerated reliability testing (typically done at high fields), it is critical that the breakdown mechanism under testing conditions is also the dominant mechanism under operating conditions. Some of the key models that are commonly used for TDDB lifttime projection[1] from accelerated testing at high fields are summarized in Figure 1.

Model	Lifetime	Mechanism
E	$A_E \exp(-\gamma_E E)$	Field assisted bond breakage
1/E	$A_{IE} \exp(-\gamma_{IE} / E)$	Fowler-Nordheim injection
Root E	$A_{RE} \exp(-\gamma_{RE} E^{1/2})$	Poole-Frenkel or Schottky
Power Law	$A_{PL} V^{-n}$	Very thin dielectrics (<4nm)

Figure 1. Commonly used lifetime models. Temperature dependence has been suppressed for purposes of clarity

In Figure 1, A is a pre-exponential factor, E represents the applied electric field, γ represents the field acceleration factor, and n the power law exponent (which can be connected to the Weibull tail of the lifetime distribution[2]). Typical electron injection mechansms include Schottky emission and Fowler-Nordheim (FN) tunneling and transport in conduction band (CB) of dielectric is Poole-Frenkel (PF) in presence of traps. Carrier heating in CB and thermalization can lead to formation of additional traps in the dielectric eventually forming a leakage path (percolation). In the regime of operating voltages of order 1-3V, the carrier heating mechanisms can become negligible and FN injection is not possible if operating voltage is less than conduction band offset of the metal-dielectric which is of order 3.5V for a metal in mid-gap of Silicon. On the other hand accelerated testing above about 3.5V necessarily has an F-N component even though the mechanism is inoperative at operating voltages. The trap creation by hot carriers injected into CB leading to wearout is a nuisance in high voltage testing and becomes negligible at operating voltages. Additionally, in scaled BEOL with high aspect ratios and thin barriers, copper can be injected into porous dielectrics electro-chemically through weak spots in the barrier at low voltages, especially in the presence of moisture. The injected copper can get reduced at the cathode and form a filamentary short. This extrinsic mechanism can be a reliability concern and must be understood and quantified.

Key to the model framework developed in this paper are several experimental observations suggesting this potentially new failure mechanism at low voltages involving copper ion and moisture. Space charge limited current studies have shown ionic transport of copper in SiO_2[3] and low-k[4]. More significantly, cyclic voltametry experiments have shown anodic copper injection[4,5] and evidence that these dielectrics can behave as solid electrolytes. Conductive bridge random access memory (CBRAM) experiments[6] have elucidated a critical role of moisture. This memory cell has a copper anode, an inert cathode like Pt and a solid electrolyte like Cu doped SiO_2. When Cu anode is biased positive, Cu ions dissolve and migrate to cathode where they get reduced and subsequently form Cu filament shorting the 2 electrodes (low resistance state). On polarity reveral, the filament breaks leading to high resistance state. This filament formation does not occur

without the presence of moisture. These experiments suggest that in scaled BEOL technologies with thin barriers, such filamentary mechanism can be an extrinsic TDDB mechanism of concern is low voltage regime.

In this paper, we investigate extrinsic reliability in low voltage regime where electro-chemical redox reactions are possible. We depict a physical model shown in Figure 2 that includes anodic copper dissolution, copper ion drift diffusion, cathodic reduction and subsequent nucleation and growth including the effect of moisture. We present analytic solution for simple limiting cases that show TDDB lifetime dependence on voltage or electric field depending on relative rates of electrode reactions and field assisted ion transport.

II MODEL FEATURES

We now present filamentary breakdown TDDB model features with the aid of Figures 2 and 3. We assume a single electrochemical reaction

$$Cu \Leftrightarrow Cu^{2+} + 2e$$

Since the divalent Cu^{2+} ion is favored in most aqueous and solid electrolytes compared to the monovalent Cu^{2+} ion often found in ionic solids[7]. In Figure 2, Cu^{2+} injection at the anode is assumed to occur at barrier weakspots based on experimental observations[4]. Drift-diffusion mechanisms transport the Cu ion to the cathode where they get reduced to Cu atoms. Clustering kinetics of Cu adatoms on foreign cathode surface (barrier) lead to the formation of a stable nucleus that grows to form a dendrite. The electrostatics and ionic transport are modeled and electrode kinetics are modeled in the spirit of discussion by Biesheuvel etal[8]. The electrical double layer[9] structure is shown in Figure 3, where near each electrode is a space charge region. The electron charge transfer reactions occur at the edge of the Stern layer, a region that acts like a dielectric.

The Butler-Volmer kinetics at the anode, for example , is given by

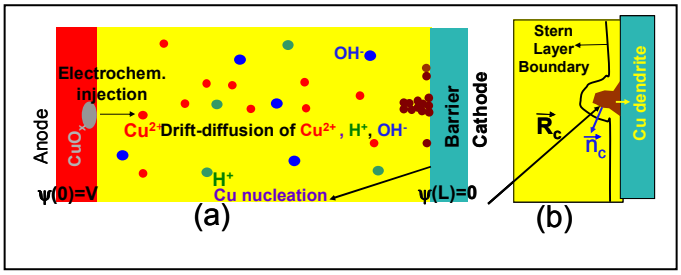

Figure 2: (a) Electrochemical TDDB model involving anodic Cu dissolution, drift-diffusion, cathodic reduction and nucleation and (b) cathode post dendrite formation with Stern layer wrapping around. The unit normal and position vector are shown at a point.

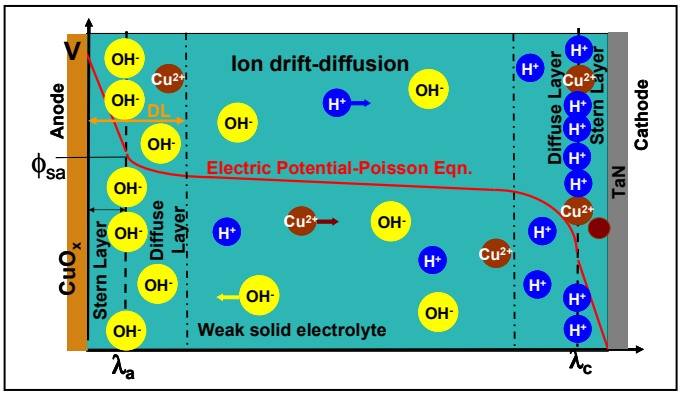

Figure 3: Electochemical aspects including electrical double layer structures at both electrodes and electrochemical charge transfer reactions at the Stern layer boundary described by Butler-Volmer Frumkin, kinetics[8].

$$i = i_{0a}\left(\exp\frac{\alpha_a \eta e}{kT} - \exp-\frac{(1-\alpha_a)\eta e}{kT}\right) \qquad [1a]$$

,where i_{0a} is the anodic exchange current density (equal oxidation and reduction current at electrode in equilibrium), η is the over-potential and *kT/e* is the thermal voltage (about 25mV at room temperature) and α_a is the transfer coefficient at the anode (typically about 0.5). As noted long ago by Frumkin, the over-potential should be defined locally at the inner part of the double layer where charge transfer occurs, and not across the full double layer including the full space charge layer as usually assumed. Building on early models of solid electrolytes[10-11], this concept has recently been incorporated into mathematical models of metal/electrolyte charge-transfer reactions[8,12-14], where the over-potential is consistently is defined as

$$\eta = \Delta\phi - \Delta\phi_e \qquad [1b]$$

where the first term is the actual potential drop across the Stern layer (surface minus electrolyte) and the second term is the equilibrium Nernst potential corresponding to the ionic concentration at edge of Stern layer. For positive over-potentials, the anodic reaction represented by the first term in equation [1a] dominates leading to Cu^{2+} dissolution at the anode whereas the second term in [1a] depicting reduction of Cu^{2+} to Cu at the same electrode becomes less insignificant. Also as the over-potentail bexomes more positive, the electrode current is predicted to increase exponentially in the so called 'Tafel Regime' of Butler-Volmer kinetics.

For modeling Cu filament growth we assume quasi-steady state hypotheses for electrostatics and boundary conditions for ions. In other words attainment of the electrostatic equilibrium and steady electrode kinetics is fast on timescale of nucleation and growth of dendrite. The Poisson to characterizes electrostatics is given by

$$\frac{d^2\psi(\vec{r},t)}{dx^2} = -\frac{\rho(\vec{r},t)}{\varepsilon_{LK}} \quad [2]$$

where ψ is the electrical potential, ρ is the total charge density and ε_{LK} is the permittivity of the low-k material and is subject to the boundary conditions

$$\psi(\vec{A},t) = V, \psi(\vec{C},t) = 0 \quad [3]$$

where *A* and *C* represent the set of points at the anode and cathode respectively.

The total charge density includes mobile ions and fixed charges in the dielectric and is given by

$$\rho(\vec{r},t) = e(2c_{Cu^{2+}} + c_{H^+} - c_{OH^-} - c_{SiO^-}) \quad [4]$$

In the above *c(r,t)* denotes concentration and *e* represents the electronic charge. Mass conservation for mobile ions is described by the continuity equation (with drift and diffusion) where it has been assumed that Cu^{2+} ions undergo no changes in the dielectric as they migrate to the cathode an assumption

$$\frac{\partial c_{Cu^{2+}}(r,t)}{\partial t} + \nabla \cdot J_{Cu^{2+}} = 0 \quad [4a]$$

valid when the voltage is small and electron fluence in the conduction band of dielectric is negligible. The flux is expressed by the Nernst-Planck equation

$$J_{Cu^+} = -D_{Cu^{2+}}(\nabla c_{Cu^{2+}} + \frac{2c_{Cu^{2+}}F}{RT}\nabla\psi) \quad [4b]$$

where, Einstein relation relating diffusivity to mobility ($D=\mu kT/e$) has been used. In the above, *R* is the universal gas constant and *F* is the Faraday constant. The quasi-steady state boundary condition (BC) for Cu^{2+} ions at the anode and cathode represents a balance between the rate of over-potential dependent electrochemical reaction and transport of ions from the Stern layer edge. In 1-D (nucleation stage), these boundary conditions are given by

$$-D_{Cu^{2+}}\frac{dc_{Cu^{2+}}(\lambda_a)}{dx}) + 2\mu_{Cu^{2+}}c_{Cu^{2+}}E = \frac{i_{0a}}{2F}\left(\exp\frac{\alpha_a\eta e}{kT} - \exp-\frac{(1-\alpha_a)\eta e}{kT}\right) \quad [5a]$$

$$-D_{Cu^{2+}}\frac{dc_{Cu^{2+}}(L-\lambda_c)}{dx}) + 2\mu_{Cu^{2+}}c_{Cu^{2+}}E = \frac{i_{0c}}{2F}\left(\exp-\frac{\alpha_c\eta e}{kT} - \exp\frac{(1-\alpha_c)\eta e}{kT}\right) \quad [5b]$$

As the the reaction rate on the left-hand side is potential dependent while the transport term on the right-hand side is electric field dependent, the TDDB lifetime is expected to have in general dependence on both factors. The rate of Cu^{2+} arrival at the cathode surface point, R_c, that determines the local nucleation rate, *R*, is given by

$$R(\vec{R}_c,t) = -D_{Cu^{2+}}\vec{n}_c \cdot \nabla c_{Cu^{2+}} - 2\mu c_{Cu^{2+}}\vec{n}_c \cdot \nabla\psi \quad [6a]$$

In the above, the quantities are evaluated at the edge of the Stern layer corresponding to R_c which is given by, S_c,

$$\vec{S}_c = \vec{R}_c + \vec{n}_c\lambda_c \quad [6b]$$

where n_c is unit outer normal to the surface at that point and λ_c is the Stern layer thckness at the cathode. The continuity equations for H+ and OH^- ions additionally involve the net rate of generation from a consideration of water-dissociation equilibrium. Silanol dissociation kinetics that determines fixed charge from on dielectric grain boundaries depends on proton concentration. The continuity equation for the mobile species H^+, OH^- and water (w) are given b

$$\frac{\partial c_i(r,t)}{\partial t} + \nabla \bullet J_i = G_i, i = H^+, OH^-, w \quad [7a]$$

Where, G_i, is net rate of generation of species *i* by chemical reactions. In equation [7a], the fluxes are given by

$$J_i = -D_i(\nabla c_i + \frac{c_i z_i F}{RT}\nabla\psi) \quad [7b]$$

Where, z_i is the valency of species *i* (0 for water). Reflective boundary conditions are assumed for other species in the absence of other electro-chemical reactions. Thus,

$$n_a \cdot J_i(\vec{R}_a + \vec{n}_a\lambda_a, t) = n_c \cdot J_i(\vec{R}_c + \vec{n}_c\lambda_c, t) = 0 \quad [8]$$

Where, R_c and R_a denote points on cathode and anode respectively, and n_c and n_a are the outward unit normals to the surface at the corresponding points. More generally, as other electro-chemical reactions occur (for example H^+ ion reduction at cathode), the reflective BC is replaced by BCs analogous to [5a] and [5b].

We now consider chemical reactions for the generation term, G_i, in equation [7a]. A water or moisture dissociation reaction is assumed[15]

$$H_2O \underset{k_{-1}}{\overset{k_1}{\Leftrightarrow}} H^+ + OH^- \quad [9]$$

In which k_1 and k_{-1} are the forward and backward rate constants. Additionally, the charge on immobile silanol groups in the low-k dielectric region is described by[16-17]

$$SiOH \underset{k_{-2}}{\overset{k_2}{\Leftrightarrow}} SiO^- + H^+$$

where H^+ is mobile proton but the other 2 species are fixed in space. Thus generation rates are given by

$$G_{H^+}(r,t) = k_1 c_w - k_{-1} c_{H^+} c_{OH^-} + k_2 c_{sil} - k_{-2} c_{H^+} c_{SiO^-}$$

$$G_{OH^-}(r,t) = k_1 c_w - k_{-1} c_{H^+} c_{OH^-} \quad [11]$$

$$G_w(r,t) = -k_1 c_w + k_{-1} c_{H^+} c_{OH^-}$$

where the concentrations refer to location r at time t. To complete the description, we need evolution rates of fixed species *SiOH* and SiO^- which are given by

$$\frac{dc_{SiOH}(r,t)}{dt} = k_{-2} c_{SiO^-}(r,t) c_{H^+}(r,t) - k_2 c_{SiOH}(r,t) \quad [12a]$$

$$\frac{dc_{SiO^-}(r,t)}{dt} = k_2 c_{SiOH}(r,t) - k_{-2} c_{SiO^-}(r,t) c_{H^+}(r,t) \quad [12b]$$

The initial conditions required to complete the formutalion are

$$c_j(r,0) = c_j(r), j = Cu^{2+}, H^+, OH^-, w, SiOH, SiO^- \quad [13$$

In many situations, especially involving slow degradation phenomena, all of these bulk electrochemical reactions are fast compared to ion transport and electrode kinetics and can be considered to be in local quasi-equilibrium. In that case, equations [11]-[13] are replaced by algebraic equations equating the product of the concentrations in each reaction with the corresponding equilibrium constant[15]. This is a significant simplification of the model, since it removes many kinetic parameters and disparate time scales for reactions. It also leads to an excellent description of experimental data for copper electrodeposition/dissolution in porous silica[16].

III TWO LIMIING CASES

The complete model given by equations [1]-[13] and additionally cathodic nucleation and growth kinetics is complex and must be numerically solved (by kinetic Monte-Carlo to capture random dendrite shapes).

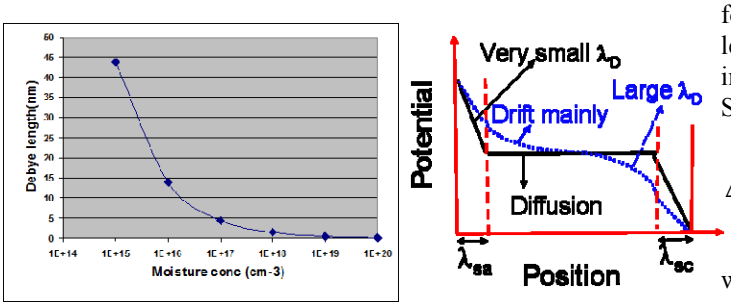

Figure 4: Debye length as a function of moisture concentration assuming complete dissociation (left) and qualitative impact on transport for low and high moisture concentration (right).

In this paper, we look at two simple limiting cases that enable an analytic solution and show the richness of behavior in the model. We look at nucleation limited lifetime case representing the situation that takes a long time to form a stable nucleus at the cathode but subsequent growth of the stable nucleus is fast. The nucleation limitation is a situation of low Cu^{2+} ion arrival rate at cathode and when nucleation occurs on a foreign non-wetting surface (in this case the barrier layer). The nucleation stage is essentially one dimensional. Once a stable nucleus forms leading to a dendrite, the problem becomes 3 dimensional as the dendrite forms a virtual cathode bending field lines. Further we consider the low moisture regime that to neglect the effects of chemical reactions described by equations [9] and [10] and consider only Cu^{2+} as the relevant species. Thus moisture is assumed to be adequate to trigger the electro-chemical mechanism and ionic strength in low-k is so small that it does not affect the electrostatic potential much. An added simplification in this nucleation limited lifetime is that quasi-steady state can apply to Cu^{2+} continuity.

The nucleation rate is given by[18]

$$J_0 = \alpha_* R \left(\frac{R}{\nu N_0}\right)^{n^*} \exp\left(\frac{(n^*+1)E_{des} - E_{sd}}{kT}\right) \exp\left(\frac{E_*}{kT}\right)$$

where. R is cathodic arrival rate, n^* is the critical size for atomistic nucleation (typically 1-10 atoms), E_{des} is desorption energy from the surface, E_{sd} is activation energy for surface diffusion, N_o is number of surface binding sites and α_* and E_* are respectively, the number of ways to form an n^*+1 cluster from an n^* cluster and E_* is the binding energy of critical cluster. Lumping material specific properties together including the valency of Cu^{2+}, the above can be written as

$$J = A_1(T) R^{(n^*+1)} = A_1(T)(i/F)^{n^*+1}$$

where i is the ionic current density and F is the Faraday constant. Thus, the steady state nucleation rate can be determined from the arrival rate of Cu atoms at the cathode. We simplify the potential profile with a piecewise linear approximation as shown in Figure 5. This assumption is valid for OH^- and H^+ ionic strengths of $< 10^{16}$ cm^{-3} or $> 10^{18}$ cm^{-3} for 20nm electrode separation as can be seen from Debye lengths shown in Figure 4. For the low moisture case of interest in most TDDB situations, the anodic voltage drop in Stern layer is given by

$$\Delta\phi_{sa} = \frac{\kappa_{lk}\kappa_{sc}\lambda_{sa}V}{\kappa_{sa}\kappa_{sc}L - \lambda_{sa}\kappa_{sc}(\kappa_{sa}-\kappa_{lk}) - \lambda_{sc}\kappa_{sa}(\kappa_{sc}-\kappa_{lk})}$$

where, κ represents material relative permittivities, L electrode separation, V the applied volotage and λ the Stern layer thickness. The subscripts *lk*, *sa*, and *sc* respectively represent low-k, Stern layer at anode and cathode. We now consider 2 situations a)Cu ion injection limited lifetime and b)Cu ion transport limited lifetime.

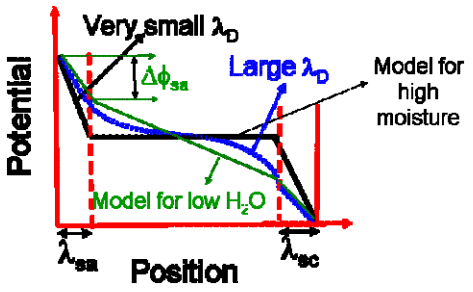

Figure 5: Piece-wise linear approximation of potential profile between cathode and anode for low and high ionic concentration of OH^- and H^+

As the over-potential is decreased, the injection rate of copper decreases exponentially but the drift velocity decreases only approximately linearly. Thus at the lower overpotentials, injection becomes limiting . Neglecting the reverse reaction for positive over-potentials, the cathodic Butler-Volmer-Frumkin injection rate from equation [1a] is given by

$$i = i_{oa} e^{\frac{\alpha_a F(\Delta\phi_{sa} - \Delta\phi_{sa,eqb})}{RT}} = i_{oa} C(T) e^{\frac{\alpha_a F \Delta\phi_{sa}}{RT}}$$

Introducing the piecewise linear approximation for the $\Delta\phi_{sa}$

$$i = i_{oa} C(T) e^{\frac{\alpha_a F \delta V}{RT}}$$

where

$$\delta = \frac{\kappa_{sc}\kappa_{lk}\lambda_{sa}}{\kappa_{sa}\kappa_{sc}L - \lambda_{sa}\kappa_{sc}(\kappa_{sa} - \kappa_{lk}) - \lambda_{sc}\kappa_{sa}(\kappa_{sc} - \kappa_{lk})}$$

and

$$C(T) = e^{\frac{\alpha_a F \Delta\phi_{sa,eqb}}{RT}}$$

Since lifetime is given by *1/(JA)* where *J* is the arrival flux and *A* is electrode area, the nucleation limited lifetime in injection limited regime is given by

$$\tau = \frac{1}{A_1(T)A}\left(\frac{F}{i_{0a}C(T)}\right)^{n^*+1} e^{\frac{(n^*+1)\alpha_a F \delta V}{RT}}$$

and lifetime depends exponentially on V. This is valid as long as V is large enough that over-potential is positive and cathodic reaction can be neglected at the anode. For the lowest positive overpotentials one can expand the exponentials in [1a] in Taylor series and show that for α_a=0.5 (a good approximation) that

$$\tau \propto \frac{1}{V}$$

We now consider the transport limited case. As the overpotential or voltage is raised, the reaction rate becomes much faster than the transport rate and the Cu^{2+} concentration at the Stern layer edge increases to reduce the overpotential for injection. As over-potential is increased further, the Cu^{2+} concentration at Stern layer edge is assumed to reach a solubility limit, c_{Cu}^* and the arrival rate to cathode is given in terms of the drift velocity v_d, in the bulk low-k by

$$R = c^*_{Cu^{2+}} v_d = 2c^*_{Cu^{2+}} \mu_{Cu^{2+}} \omega E$$

where

$$\omega = \frac{\kappa_{sc}\kappa_{sa}}{\kappa_{sa}\kappa_{sc} - \lambda_{sc}[\kappa_{sa}(\kappa_{sc} - \kappa_{lk})/L] - \lambda_{sa}[\kappa_{sc}(\kappa_{sa} - \kappa_{lk})]}$$

The nucleation rate becomes

$$J = A_1(T)R^{n^*+1} = A_1(T)[2\mu_{Cu^{2+}} c_{Cu^{2+}} \omega E]^{(n^*+1)}$$

Hence the nucleation limited lifetime in this limit is given by

$$\tau = \frac{1}{JA} = \frac{1}{AA_1(T)}\left(\frac{1}{2\mu_{Cu} c^*_{Cu} \omega E}\right)^{n^*+1}$$

and the nucleation limited lifetime exhibits power-law dependence on E. In the above expressions, E, is the average electric field given by 1/V.

IV GENERALIZATION TO HIGHER VOLTAGES

The range of voltages of interest in TDDB is from 1-3V (operating condirions) to about 15V (accelerated testing). Assuming low moisture, a line to line spacing of 20nm and Stern layers 1nm thick, the voltage drop in SL is about 0.05-0.15V under operating conditions to about 0.75V during accelerated testing. At room temperature, this spans a range of about 2-30 times the thermal voltage. A signature of Butler-Volmer kinetics is the linear dependence of the logarithm of current for larger positive and negative over-potentials (Tafel regime). This model predicts incredibly large reaction rates and negligible charge-transfer resistance for typical large voltages, and thus must be corrected in order to make realistic predictions of TDDB

As the over-potential is increased, ion transport limitation and the occurrence of other electro-chemical reactions can lead to deviations from Tafel behavior. In nanoscale electrolyte layers between metal electrodes, diffusion limitation is easily reached[12] and then exceeded by the formation of extended non-equilibrium space charge, in both steady[13] and unsteady[14]

situations, and these phenomena can be strongly influenced by water splitting and membrane charge regulation[15].

At high voltages, another fundamental limitation on electrode reaction rates is predicted by Marcus's theory of electron transfer reactions[19,20,21-23], which has recently been shown to replace Butler-Volmer kinetics as the proper description of metal/insulator charge-transfer reactions in Li-ion. According to this theory, electron transfer (for example in an oxidation reaction) can occur only when the atomic configuration in the polar environment is modified to facilitate the electron transfer. Energy is needed to create a solvent environment where electron transfer can adiabatically take place (transition state) and this is the energy of activation. A re-organizational energy . λ, is defined as the energy required to deform the reaction coordinate of the reactant to that of product without permitting electron transfer and is dominated by electrostatic effects of dielectric relaxation. Remarkably, this theory shows that the electrode kinetics is maximum when the free energy difference between the reactant and product (a negative quantity) is just equal to the re-organizational energy (positive). Making the free-energy more negative beyond this point reduces the electrode reaction rate. Since the free-energy is directly proportional to the over-potential (aside from Nernst concentration terms[23]),, Marcus's theory predicts that the electron transfer kinetics first increases exponentially with over-potential, reaches a maximum and subsequently decreases– the opposite voltage dependence predicted by the empirical Butler-Volmer equation.

For electron transfer reactions at metal electrodes (electo-chemical reactions), the electron transfer kinetics should take into account the Fermi-Dirac statistics for electron distribution in electrode states. Chidsey's analysis[24] shows that the one does not observe the Marcus inverted region atleast for moderate overpotentials, but, rather, current saturating. The qualitative trends are depicted in Figure 6.

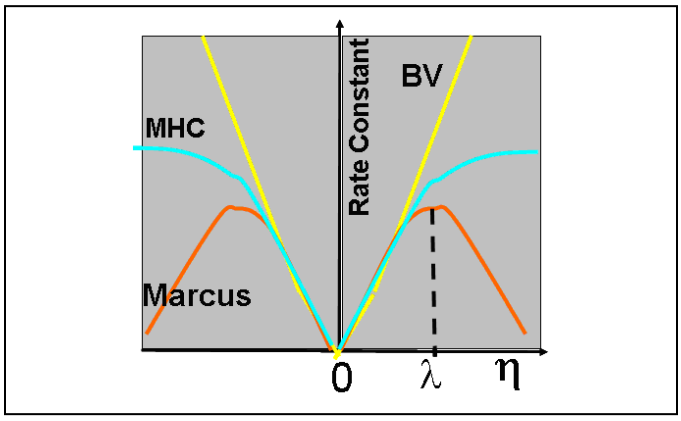

Figure 6: Qualitative characteristics of Butler-Volmer (BV), Marcus and Marcus-Hush-Chidsey (MHC) kinetics. The Marcus rate peaks when the over-potential is same as the reorganizational energy, λ. MHC kinetics shows saturation beyond λ.

Electron transfer theory has significant implications for TDDB testing. At typical accelerated testing voltages (several times the thermal voltage), electrode kinetic reactions may become small or saturate but intrinsic wearout mechanism of Fowler-Nordheim injection and Poole-Frenkel mechanism will be significant. However in the operating voltage regime (~ 1-3V), the electrode kinetics can be significant compared to the intrinsic wearout mechanism which would have been reduced significantly. This raises the question on the validity of high voltage testing and extrapolation to operating voltages.

The generalization of the low voltage limit model presented in this paper to higher voltages needs the incorporation of Marcuss-Hush-Chidsey (MHC) kinetics[22-24] for the boundary conditions [5a-5b] instead of Butler-Volmer kinetics. The validity of this approach is strongly suggested by very recent experimental results on Li-ion batteries[22]. Experiments on porous electrodes consisting of carbo-coated lithium iron phosphate nanoparticles have revealed, for the first time, that MHC kinetics is able to quantitatively predict the fundamental charge-transfer rate, based on a mechanism of electron transfer from the metallic carbon coating to the iron redox site in the poorly conducting, low-k iron phosphate solid electrolyte. In this new mechanism, the lithium ion is exchanged quickly across the interface, after the rate-limiting step of electron transfer occirs. Similar physics may govern the electodeposition and dissolution of copper in silica or other low-k materials in TDDB or CB-RAM applications.

V CONCLUSIONS

In conclusion we have presented an electro-chemical picture for TDDB failure in scaled BEOL that can occur in the operating voltage regime. The model in general has V and E dependence and we have shown limiting cases that show dependence on only V or E. The model can be generalized to higher voltages where extrinsic and intrinsic mechanisms occur concomitantly. The intrinsic wearout mechanism described in Hasse[25] must be added to the electr-chemical mechanism described in this paper. Further, other electr-chemical reactions can come into play. Recently, Kong Boon Yeap et al[26] have tried reported by electrical, chemical and physical analysis that they do not observe Cu ion injection below 200C in their experiments with porous low-K material. A possible explanation is absence of moisture in their experiments, key for electro-chemical mechanism[6]. This result contradicting some other results[3-5] emphasizes the need to understand and characterize the injection kinetics at the electrode, possible electrode reactions and their dependence on barrier thickness, temperature, humidity and bias.

ACKNOWLEDGEMENT

The authors acknowledge discussions with B. Li, M. Krishnan, B. Linder, E. Wu, C. Witt, A. Sahin, J. Stathis and L. T. Romankiw. The authors acknowledge inputs and discussions with mentor for this paper, Kong Boon Yeap (Global Foundaries)

REFERENCES

[1] J. W. Mcpherson, Reliability Physics and Engineering, Springer Verlag New York, 2010, pp 166-173

[2] J.-L. Le, Z. P. Bazant, and M. Z. Bazant, 'Lifetime of high-k gate dielectrics and analogy with strength of quasi-brittle structures', J. Appl. Phys. 106, 104119 (2009).

[3] B. G. Willis and D. V. Lang., "Oxidation mechanism of ionic transport of copper in SiO_2 dielectrics", Thin Solid Films 467, pp 284-293 (2004)

[4] L. S. Chen et al..,"Observation of space charge limited current by copper ion drift in porous low-k/Cu interconnects" Applied Physics Letters 96, pp 090913. 46-53 (2010)

[5] Tappertzhofen, et al., 'Nanoionic transport and electrochemical reactions in resistively switching silicon dioxide', Nanoscale 4. pp. 464-475 (2012)

[6] T. Tsuruoka et al., Adv. Funct. Mater. 22, pp 70-77, (2012)

[7] C. Leger, F. Argoul and M. Z. Bazant, `Front dynamics during diffusion-limited corrosion of ramified electrodeposits', J. Phys. Chem. B 103, 5841-5851 (1999).

[8] P. M. Biesheuvel, M. van Soestbergen and M. Bazant, 'Imposed currents in galvanic cells', Electrochima Acta 54, pp 4857-4871, (2009)

[9] A. C. Fisher, Electrode Dynamics, Oxford New York, 1996

[10] E. M. Itskovich, A. A. Kornyshev, and M. A. Vorotyntsev, `Electric current across the metal-solid electrolyte interface. I. Direct current, current-voltage characteristic', Phys. Stat. Sol. (a), 39, 229-238 (1977).

[11] A. A. Kornyshev and M. A. Vorotyntsev, Conductivity and space charge phenomena in solid electrolytes with one mobile charge carrier species: A review with original material, Electrochim. Acta, 26, 303-323 (1981).

[12] M. Z. Bazant, K. T. Chu and B. J. Bayly, `Current –voltage relations for electrochemical thin films', SIAM J. Appl. Math 65, 1463 (2005).

[13] K. T. Chu and M. Z. Bazant, `Electrochemical thin films at and above the classical limiting current', SIAM J. Appl. Math. 65, 1485 (2005).

[14] M. van Soestbergen, P. M. Biesheuvel, and M. Z. Bazant, `Diffuse-charge effects on the transient response of electrochemical cells,' Phys. Rev. E 81, 02153 (2010).

[15] M. B. Andersen et al., PRL 109, 108301 (2012).

[16] Behrens, S. H.; Grier, D. G. The charge of glass and silica surfaces. J. Chem. Phys. 115, 6716−6721 (2001).

[17] Gentil, C.; Co□te, D.; Bockelmann, U. Transistor based study of the electrolyte/SiO2 interface. Phys. Status Solidi A 203, 3412−3416 (2006).

[18] I. Markov, 'Crystal Growth for Begineers', World Scientific, Singapore

[19] R. A. Markus, ' Electron transfer reactions in chemistry. Theory and experiment', Reviews in Modern Physics 65, No 3, pp 599-610, 1993.

[20]A. Nitzan, 'Chemical Dynamics in Condensed Phases : Relaxation, Transfer and Reactions in Condensed Molecular Systems, ' Oxford University Press, New York, pp 551-570, 2006.

[21] A. M. Kuznetsov and J. Ulstrup, *Electron Transfer in Chemistry and Biology: An Introduction to the Theory* (Wiley, 1999).

[22] P. Bai and M. Z. Bazant, Charge transfer kinetics at the solid-solid interface in porous electrodes , Nature Communications, 5:3585 (2014).

[23] M. Z. Bazant, `Theory of chemical kinetics and charge transfer based on nonequilibrium thermodynamics', Accounts of Chemical Research 46, 1144-1160 (2013).

[24] C. E. D. Chidsey, 'Free Energy and Temperature Dependence of Electron Transfer at the Metal-Electrolyte Interface', Science 251, pp919-922, 1991.

[25] G. Haase, 'A model for dielectric degradation of interconnect low-K dielectrics in microelectronic integrated circuits,' J. App. Phys. 105, 044908, 2009.

[26] Kong Boon Yeap et al., 'In-situ Study on Low-k Interconnect Time-Dependent Dielectric Breakdown Mechanism', J. App. Phys. 115, 124101, 2014.